Rewiring of mite allergen-specific Th-memory-associated gene networks during immunotherapy

Running head: Systems level analyses of immunotherapy mechanisms

Authors

Anya C. Jones PhD[1], Denise Anderson MBiostat[1], Niamh M. Troy BSc[1,2], Dominic Mallon MBBS[4], Rochelle Hartmann RN[4], Michael Serralha BSc[1], Barbara Holt BSc[1], Anthony Bosco PhD[1,#], Patrick G. Holt DSc[1,3,#]

Affiliations

[1]*Telethon Kids Institute, The University of Western Australia.*

[2]*School of Medicine, The University of Western Australia, Perth, Australia.*

[3]*Child Health Research Centre, The University of Queensland, Brisbane, Australia.*

[4]*Dept of Clinical Immunology, Fiona Stanley Hospital, Perth, Australia*

[#]Joint senior authors.

Corresponding author

Prof Patrick G. Holt

Telethon Kids Institute

Northern Entrance, Perth Children's Hospital

15 Hospital Avenue, Nedlands WA 6009

Telephone: +61 8 6319 1412

Fax: +618 6319 1777

Email: Patrick.Holt@telethonkids.org.au; Marina.Stubbs@telethonkids.org.au

Funding sources

Supported by funding from ALK Abello, Horsholm, Denmark, and the National Health and Medical Research Council of Australia. AB is supported by a Fellowship from the Simon Lee Foundation. NMT is supported by Asthma Australia Mickie Hardy PhD Scholarship.

Conflicts of interest

The authors declare no conflict of interest.

PGH conceptualised the study. ACJ, DA and BH contributed to data analysis. AJC, DM, AB and PGH contributed to data interpretation. NMT, DM, RH, MS and BH contributed to data collection/curation. ACJ, AB and PGH contributed to paper writing.

ABSTRACT

Background

Multiple regulatory mechanisms have been identified employing conventional hypothesis-driven approaches as contributing to allergen-specific immunotherapy outcomes, but understanding of how these integrate to maintain immunological homeostasis is incomplete.

Objective

To explore the potential for unbiased systems-level gene co-expression network analysis to advance understanding of immunotherapy mechanisms.

Methods

We profiled genome-wide allergen-specific Th-memory-associated responses prospectively during 24mths subcutaneous immunotherapy (SCIT) in 25 rhinitics, documenting changes in immunoinflammatory pathways and associated co-expression networks and their relationships to symptom scores out to 36mths.

Results

Prior to immunotherapy, mite-specific Th-memory-associated response networks involved multiple discrete co-expression modules including those related to Th2-, Type1-IFN-, Inflammation-, and FOXP3/IL2-associated signalling. A signature comprising 109 genes correlated with symptom scores, and these mapped to cytokine signalling/T-cell activation-associated pathways, with upstream drivers including hallmark Th1/Th2- and inflammation-associated genes. Reanalysis after 3.5mths SCIT updosing detected minimal changes to pathway/upstream regulator profiles despite 32.5% symptom reduction, however network analysis revealed underlying merging of FOXP3/IL2- with Inflammation- and Th2-associated modules. By 12mths SCIT, symptoms had reduced by 41% without further significant changes to pathway/upstream regulator or network profiles. Continuing SCIT to 24mths stabilised symptoms at 47% of baseline, accompanied by upregulation of the Type1-IFN-associated network module and its merging into the Th2/FOXP3/IL2/Inflammation module.

Conclusions

SCIT stimulates progressive integration of Th-memory-associated Th2-, FOXP3/IL2-, Inflammation-, and finally Type1-IFN-signalling subnetworks, forming a single highly integrated co-expression network module, maximising potential for stable homeostatic control of allergen-specific Th2

responses via cross-regulation. Th2-antagonistic Type1-IFN signalling may play a key role in stabilising clinical effects of SCIT.

Key words

Immunotherapy, $CD4^+$ Th-memory cells, inhalant allergy, rhinitis, network analysis

Abbreviations

Subcutaneous immunotherapy (SCIT), specific immunotherapy (SIT), peripheral blood mononuclear cells (PBMC), weighted gene coexpression network analysis (WGCNA), differentially expressed genes (DEG), upstream regulator analysis (URA), bacterial lipopolysaccharide (LPS).

INTRODUCTION

The primary aim of allergen-specific immunotherapy (SIT) is attenuation of downstream inflammation resulting from allergen-specific $CD4^+$Th-memory cell activation. Multiple regulatory mechanisms are believed to contribute to SIT-induced modulation of Th-memory-dependent inflammatory symptoms[1-4], but the understanding of how these operate individually/collectively is relatively scant. Traditional approaches to this question have emphasised hypothesis-driven studies on candidate targets selected based on *a priori* knowledge, focusing on relatively limited numbers of effector/regulatory mechanisms. However, it is now recognised that immune responses, including those induced by allergens[5,6], involve thousands of genes functioning within complex networks, and hence the application of systems-level analytical methodology which can capture and deconvolute some of this complexity may prove useful in elucidating SIT mechanisms.

In this regard, our group has previously employed genome wide expression profiling of allergen-activated $CD4^+$T-cells to define a highly inter-correlated Th2-associated gene subnetwork that is operative in atopic children at risk of allergic disease[5-7]. In the analyses below we have extended this systems-level approach, to identify the full spectrum of functionally coherent gene subnetworks operating within aeroallergen-specific Th-memory-associated responses in highly symptomatic adults, and to map changes in their architecture and interconnectivity during two years of SIT, in particular changes associated with reduction in Th2-associated allergy symptoms.

METHODS

Study population

House dust mite (HDM) sensitised subjects (SPT^+ and/or specific IgE ≥0.35kU/L) with perennial rhinitis (n=25; **Table E1**) were recruited at Fremantle Hospital, Western Australia, prior to commencement of a standard 3yr course of HDM-specific subcutaneous immunotherapy (SCIT). The SCIT protocol and mechanistic study design was approved by the institutional ethics committee, and consent obtained from all subjects.

Immunotherapy protocol

The protocol was based on Blumberga[8], utilising Alutard® SQ *Dermataphagoidies pteronyssinus* (ALK, Horsholm, Denmark). Treatment included 15-week updosing (up to 100,000 SQ-U) and 3-year maintenance with injection intervals of 6±2 weeks; patients recorded daily respiratory symptoms and medication use, the details of which were utilised to generate symptom scores at the end of designated treatment periods[9].

PBMC processing

PBMC were collected prior to immunotherapy (Visit 1/V1), and at 3.5mths (V2), 12mths (V4) and 24mths into treatment (V5; **Figure E1**), and cryopreserved as described[10].

Analytical strategy

This exploratory study aimed to evaluate the potential of network analytic methodology to elucidate short-/long-term effects of SCIT on allergen-specific Th-memory-associated responses. Our approach (**Figure E2**) involved initial *in vitro* culture of unfractionated PBMC with unfractionated HDM allergen extract to enable interactions to occur between allergen-specific and non-specific T-cells and bystander myeloid cells. We have previously demonstrated that the overall HDM-induced Th-memory-associated response signature in atopics comprises components from both HDM-triggered and (cytokine-triggered) HDM-unresponsive CD4+T-cells[5,7], hence we purified $CD4^+$T-cells from these cultures for transcriptomic profiling without additional fractionation. Microarray analysis was used to compute T-cell differentially expressed gene (DEG) signatures, followed by pathway analysis to identify functionally coherent pathways that map to these signatures (IL2-signalling; Th2 etc). This was followed by upstream regulator analysis (URA) to identify "driver" genes in specific Th-memory cells and/or in bystander myeloid/T-cell populations in PBMC, that are statistically likely to have contributed to the 24hr T-memory-associated signatures at an earlier stage in the activation process.

Independently, network analysis was performed to identify gene coexpression networks that underpin allergen-driven Th-memory-associated responses. A subset of the subjects also received grass allergens in the SCIT mix, and sub-analysis of study outcome samples after stratification by treatment to ascertain the effects of the latter on HDM-induced DEG profiles.

In vitro cell cultures and CD4^{+}T cell isolation

PBMC from visits V1-V4 were thawed and cultured together employing the same batch of LPS-depleted whole HDM extract (10ug/ml; gift from ALK Abello) or medium control for 24h[10], whilst V5 was cultured as a stand-alone experiment employing the same reagent batches. We have previously established that the AIM-V serum-free medium employed does not support PBMC activation by LPS, including when spiking cultures with up to 100ug/L LPS[10]. CD4^{+}T cells were harvested from cultures using Dynabeads(ThermoFisher) for total RNA extraction with TRIzol(Ambion, Life Technologies) followed by RNAeasy MinElute(Qiagen, Hilde, Germany), and subsequent microarray profiling(Affymetrix PrimeView).

Antibody measurement

HDM-specific IgE and IgG4 levels were quantified by ImmunoCAP(ThermoFisher)[10].

Microarray data pre-processing and differential expression analysis

Raw microarray data are available from the Gene Expression Omnibus repository(GEO Accession #GSE122290). Gene expression data were analysed using R statistical computing software(version 3.4.4). A custom chip description file with updated genome information (primeviewhsentrezgcdf, version 22) was utilised to annotate probe sets to genes[11]. Quality control(QC) of raw microarray data was performed with *ArrayQualityMetric*s[12]; one case/control subject at V5 was removed based on QC plots. The robust multi-array average algorithm(*RMA*[13]), was used for background correction and quantile normalisation. Non-informative probe sets were filtered out using the proportion of variation accounted for by the first principal component algorithm(*PVAC*>0.4[14]), resulting in 3264 probe sets(V1, V2 and V4) and 3825 probe sets(V5) for downstream statistical analysis.

DEG were identified using *limma*[15], with a false discovery rate control for multiple testing. Quality weights were included in the linear model with the *arrayWeights*()[15] function. Paired samples were taken into account with the *duplicateCorrelation()*[15] function and the model estimates were adjusted for batch effects, which had been identified with PCA plots (**Figure E3**). We tested whether response to stimulation is associated with respiratory symptoms at each visit using *limma* by including both covariates and their interaction in the linear model.

Network analysis

Prior to network construction, raw expression data were pre-processed separately for each visit with *RMA*[13] and batch variation was removed with *ComBat*[16]. Batch effect removal was verified by PCA plots (**Figures E4/5**) and differences between HDM-stimulated and control cultures were confirmed and visualised with heatmaps (**Figure E6**). The *PVAC*-filtered data resulted in 4027, 3042, 3912 and 3831 probe sets at V1/V2/V4/V5 respectively, and these probe sets were combined resulting in 5265 genes for network analysis. Co-expression networks were constructed employing *WGCNA(*weighted gene coexpression network analysis)[17], based on the concept that the organisation and function of a biological system can be represented as a network graph of coexpressed genes. We employed the following parameters for *WCGNA*: signed networks, softPower = 11, Pearson correlation, minimum module size = 50, deepsplit = 0, merge cut height = 0.1. Principal component analysis was performed at each visit to determine the relatedness of the modules. The modules at each time point (V1, V2, V4 and V5) were examined for enrichment with differentially expressed genes (HDM stimulated versus control) obtained with *limma*. Then, HDM-response modules were identified based on median adjusted *p*-values < 0.05 (from the *limma* analysis). Network wiring diagrams were constructed utilising the top-weighted 800 network edges (pairwise gene-gene correlations), which were extracted from the adjacency matrix from the expression data. The networks were graphically depicted using Cytoscape[18] (version 3.6.1), employing the NetworkAnalyzer tool, parameters: undirected edges, organic layout, map node size to degree: low node values to small size.

Pathways analysis & Gene ontology analysis

Pathway enrichment and gene ontology analysis were performed with InnateDB version 5.4[19] based on a hypergeometric distribution and Benjamini & Hochberg corrected *P-values*≤0.05. Public databases utilised included INOH, KEGG, NETPATH, PID, BIOCARTA, REACTOME for pathways analysis and gene ontologies including molecular function, cellular component and biological process.

Upstream regulator analysis

Putative regulators of the gene expression patterns were identified employing Ingenuity Systems Upstream Regulator Analysis(URA)[20]. Molecular drivers with Benjamini & Hochberg adjusted *P-values*≤0.05 and absolute *Z-scores*≥2.0 were deemed significant. The overlap *P-value* measures enrichment and the *Z-score* measures activation/inhibition of the regulator.

RESULTS

Evolution of symptoms over time during SCIT

Figure 1 illustrates symptom scores(mean±95% CI) at each sampling. The largest drop in symptom scores had occurred by the end of the updosing phase(32.5% reduction; V2/3.5mths) at which point maintenance therapy commenced. The mean symptom score decline reached 37% by V4(12mths) and 51% by V5(24mths), remaining at this level to the end of treatment at V6(36mths). Consistent with the literature[1,2,4], reductions in symptoms across the first year of SCIT were accompanied by increases in serum HDM-specific IgE and IgG4 (**Figure E7A/B**).

$CD4^+$T cell immune responses pre-treatment

Baseline $CD4^+$T-cell responses to HDM at V1 comprised 1715 DEG (**Figure 2A/Tables E2/E3**). Pathways analysis demonstrated enrichment for genes associated with a number of functionally coherent pathways, in particular involving cytokine/chemokine receptor interactions, antigen processing/presentation and T-cell transcriptional activation (**Figure 2B**). URA revealed that the top-ranking putative drivers (ranked in **Figure 2C** by activation *Z-scores*/adjusted *P-values*) were dominated by those associated with Th1/Th2 immunity (including respectively IFNG/IL12; IL4/IL5), inflammation (TNF, IL1B, CSF2, STAT3) and T-cell activation (CD40 ligand, CD3/TCR, CD28).

Association of respiratory symptoms with gene expression pre-treatment

We tested whether allergen-driven T-cell response patterns were associated with respiratory symptom scores at each visit employing *limma*. At pre-treatment(V1) we identified a gene signature comprising 109 DEG as significantly associated with symptoms (**Figure 2D, Table E4**). Pathways analysis showed that symptom-associated genes were enriched for cytokine/cytokine-receptor interactions, Th1-/Th2-mediated signalling, calcineurin-regulated NFAT-dependent lymphocyte transcription, whilst downregulated genes were enriched for cell-cell communication/transmembrane transport (**Figure 2E**). URA demonstrated that the top-ranking drivers were associated with T-cell activation (TCR and CD3 complexes, NFATC2, CD40LG), Th1 immunity (IL12 complex/IFNG), Th2 immunity (IL4/IL5), common gamma chain signalling (IL2, IL4, IL7, IL15, IL21), and inflammation (TNF, STAT3, STAT6, IL1B, IL18; **Figure 2F**).

We then replicated the analysis from **Figure 2D**, in this case seeking to identify gene expression patterns associated cross-sectionally with attenuated post-treatment symptom expression scores at V2, V4 and V5 respectively. No significant associations were detected at these later time points, indicating that the contribution of HDM-specific immunoinflammatory responses to the overall

expression of clinical symptoms was significantly diminished from V2 onwards relative to pre-treatment (**Figure E8**).

Impact of SCIT on HDM-specific Th-memory-associated response profiles

We assessed HDM-induced T-cell response patterns at V2, V4 and V5. In excess of 1800 DEG were detected at each of these sampling times **(Figure 3A, Tables E3, 5-7**). The list of up/downregulated pathways and their putative drivers at the different visits during SCIT (**Figure 3B,C**) closely resembled that identified for V1 (**Figure 2B,C**); the notable exception was the presence of an operational/upregulated type1/2 interferon signalling pathway at V5 (**Figure 3B/C**) that was not active earlier in the time course. In particular, no type1 interferon-associated genes appeared at any level of significance amongst the list of upstream drivers prior to V5. As illustrated in **Table I,** which shows activation *Z-scores* at each visit for the V5 upstream drivers, scores for the interferon-associated drivers are uniformly elevated at V5, in contrast to the stable pattern for other drivers including those related to Th2 inflammation.

***WGCNA* analysis of the HDM-specific T-cell responses**

We next constructed weighted gene co-expression networks at each sampling to obtain a systems-level understanding of how the correlation patterns between genes changed over the course of allergen-specific immunotherapy. First, we calculated ranked expression levels and ranked network connectivity, and compared the data at V1 with subsequent visits. As illustrated in **Figure E9**, the data showed that variations in network connectivity (i.e. gene-gene co-expression patterns) were most striking at V2 and V5. These findings were reflected by conventional statistical analyses, which identified hundreds of DEG between the respective responses at V2 versus V1, and V5 versus V1 (Tables E7/E8). Variations in network connectivity were also evident at V4, even though no differentially expressed genes were identified between the respective responses at V1 and V4.

We next looked for changes in modular architecture of the co-expression networks during SCIT. To illustrate this, we superimposed the network connectivity patterns for each visit over the modular architecture from V1 (**Figure 4A**). The data showed that V2 and V5 were characterised by the presence of strong correlation patterns off the diagonal, suggesting rewiring between modules. Moreover, this was also reflected by changes in the modular architecture from V1 to V5 (indicated by colours below **Figure 4B**, left panel; and the roadmap showing the progressive re-wiring of modules (denoted A-N) at ensuing visits (**Figure 4B**, right panel). The co-expression networks were organised into 9/7/10/6 modules at V1/V2/V4/V5 respectively (**Figure 4B**). We then interrogated the modules for functional coherence and examined them for DEG enrichment (**Figure 4C**). At pre-

immunotherapy V1, the modules denoted C/F/G/I, relating respectively to metabolism of proteins/Th2 immunity/inflammation/IL2-signalling, were upregulated. Of note, type1 interferon-associated genes formed a discrete module(A), however, these were not differentially expressed in the response. Following completion of updosing at V2, the modular architecture had become restructured and the modules F, G and I amalgamated forming one upregulated module J (**Figure 4B,C**), whilst the type1 interferon network remained unchanged, and lysosome/phagosome/antigen-processing-presentation module C and TCR signalling module D were downregulated.

At V4, the IL2 signalling and Th2 networks remained fused (module L) while the inflammation/lysosome/phagosome/antigen processing-presentation (G), metabolism of proteins (C), and type1 interferon-associated (A) modules remained as discrete networks (**Figure 4B,C**). Finally at V5, the original subnetworks from V1 (F, G and I) had consolidated into a single large upregulated co-expression module (N, **Figure 4B,C**), which included re-wiring with the now upregulated interferon-associated genes which were originally within the (then quiescent) module A at V1 (**Figure 4B,C**).

To visualise these progressive changes in network structure during the course of SCIT we plotted the top 800 network edges/connectivity patterns from *WGCNA* employing Cytoscape, focusing initially on the components of the key modules A/F/G/I from V1. **Figure 5/Figure E10** illustrates the major structural changes that occurred in the network between V1 to V5, notably the merging of the initially discrete Th2-, IL2-, and Interferon-signalling modules into a single interconnected coexpression module by the end of 2yrs treatment. As shown this transition appears to involve two stages, with initial coalescing of the Th2- and IL2-signalling modules evident by the end of SCIT updosing(V2), while final merging with the Interferon module was not observed until the second year of SCIT(V5). Of note, repetition of these analyses employing other network parameters (softPower 12,13, and minimum module size=20), resulted in similar conclusions regarding network rewiring (data not shown).

We also calculated network summary statistics to identify hubs and bottleneck nodes[21] that are thought to play central roles in network stabilisation. With respect to the key V5 module N, 10 of the top 20 hub/bottleneck genes identified via Cytoscape based on the betweenness centrality and degree metrics[21] were associated with IL2/FOXP3-signalling and 4 with Type1 IFN-signalling (**Table E8**), consistent with their likely contributions to eventual consolidation of the SCIT-induced low responder phenotype.

As noted in Methods 18 of the 25 HDM allergic subjects employed here were also grass responsive, and received grass SCIT in parallel with HDM treatment. We repeated these analyses on HDM associated responses after removal of the 7 subjects who did not receive grass SCIT (**Figure E11**), and the overall HDM-associated response pattern (in particular the module consolidation at V5; **Figure E12**) was essentially unchanged.

DISCUSSION

Successful SCIT is typically a biphasic process, in which symptom improvement commences in responsive subjects within a few months and peaks within the first treatment year, however "consolidation" of the clinical effects of SCIT requires a 2nd (sometimes 3rd) year of maintenance treatment to prevent slow reversion to pre-treatment allergen-responder status[22,23]. Current understanding of the mechanism(s) underlying desensitisation derive principally from studies on the early phase of SCIT, which suggest important roles for T-regulatory cells, allergen-specific IgG4, and a broad range of other negative control mechanisms[1,2,4]. How these mechanisms interact to control allergen-induced responses in this early phase of SCIT is incompletely understood, and it is not known whether the same range of mechanisms are responsible for eventual stabilisation of the SCIT-induced low-allergen-responder phenotype, or alternatively whether additional control mechanisms are induced/recruited via more prolonged treatment. In this regard it is pertinent to note that (as in **Figure E7**) specific IgE production is maintained or transiently boosted during the early period of SCIT, and declines only slowly with continuing therapy, even in subjects with markedly reduced symptoms[1,2,24], inferring that Th2-polarised immunological memory against the target allergen is not completely abrogated by SCIT, but instead its downstream immunoinflammatory effects are attenuated.

Our principal aim in this study was to test whether unbiased systems-level analyses of HDM-specific Th-memory-associated response profiles spanning the early and later(consolidation) phases of SCIT, could provide mechanistic insight into this biphasic process. Our study yielded two sets of complimentary findings. In untreated/highly symptomatic subjects, the HDM-induced Th-memory-associated signature is enriched for multiple genes that map to pathways associated with transcriptional activation and cytokine/cytokine-receptor interactions, and the molecular drivers of this response are dominated by hallmark Th1/Th2- and inflammation-associated genes (**Figure 2A-C**) which in turn are correlated with symptom scores (**Figure 2D-F**). This correlation was lost by the end of SCIT updosing (at 3.5mths), but analysis of the accompanying "early post-treatment" HDM-specific DEG signature revealed minimal accompanying changes in underlying pathway/upstream driver profiles, and moreover this pattern did not change substantially throughout the initial course of maintenance therapy to 12mths(V4; **Figure 3B,C**), despite a further decline in symptom scores(**Figure 1**). Continuation of maintenance therapy for a second 12mth period resulted in stabilisation of symptom scores by 24mths/V5 at 51%(mean) below baseline(**Figure 1**), and the appearance in the HDM-specific response profile of upregulated IFN-signalling (**Figure 3B**; **Table I**) and Type1-IFN-associated transcriptional regulators (particularly STAT1 and IRF7; **Figure 3C**).

Additional gene co-expression analyses provide a holistic view of the overall HDM-specific Th-memory-associated response which is key to interpretation of these findings. As illustrated in **Figures 4/5/E10**, the use of *WCGNA* enables construction of complex networks comprising functional modules, each encompassing genes which are highly correlated with each other on the basis of co-expression; exemplars in **Figure 5** are modules designated respectively "Th2" which includes the core IL4/IL4R/IL5/IL9/IL13 gene signature, and "IL2-signalling" encompassing IL2/IL2R/FOXP3 and related genes. Tracking the connectivity patterns between these and other functionally coherent co-expression modules within the network across the time-course of SCIT suggests that the influence of therapy on the overall allergen-induced DEG response extends beyond quantitative effects on transcription, and importantly includes coordination/synchronisation of the expression of key sets of genes within the Th-memory-associated response.

Thus at V1(pre-treatment) at which time prominent drivers of symptoms include Th2 effectors exemplified by IL4/IL5 and archetypal inflammatory mediators such as TNF/IL1B/1L18, the network modules associated with Th2-, inflammation-, and IL2/FOXP3-signalling were isolated in the network topology, suggesting they operate relatively independently (modules F,G,I in **Figure 4B**), resulting in a low-level of coordination between the activity of inflammatory and regulatory networks in highly symptomatic subjects. However overall network topology is radically altered during the updosing phase of SCIT such that by V2 the Th2 and IL2/FOXP3 modules together with much of the inflammation subnetwork have coalesced into a single entity (module J/**Figure 4B**), suggesting enhanced coordination of expression of symptom-associated and regulatory genes/pathways, and this coincides with initial symptom decline and termination of the nexus between symptom scores and the overall Th-memory-induced DEG signature. The early SCIT-induced merging of these subnetworks persists in the face of further changes in network topology as therapy continues, culminating during the 2nd year of treatment with additional merging by V5 with the now upregulated IFN-signalling subnetwork, to form the single highly integrated module N (**Figure 4B**) encompassing coordinated Th2-, IL2/FOXP3-, inflammation-, and IFN-associated signalling. In contrast, modules B, C and D encompassing the key "infrastructural" activities (antigen processing/presentation, TCR activation, translation) which underpin the overall Th-memory-associated response, remain as distinct entities throughout.

We performed additional analyses to visualise changes in network wiring across time, with particular emphasis on gene-gene connections in network module N/V5 which encompasses the main inflammatory effector/regulatory pathways following 2yrs SCIT (**Figure 5)**. As noted in Results,

subsidiary analyses (**Table E9**) highlighted the prominence of genes associated with IL2/FOXP3-signalling in stabilising this network and hence consolidation of the clinical effects of SCIT. However additional findings in **Table E9** together with **Table I/Figures 4,5** suggest that other factors related to network topology are also involved. In particular, the upregulation during the 2nd treatment year of the initially quiescent Type1-IFN module and its "wiring" into the aeroallergen-specific Th-memory-associated co-expression network at V5, may also play a key role in this stabilisation process.

In this regard, previous studies have identified Type1-IFN-associated DEG signatures in both PBMC- and sputum-derived cellular response profiles in a variety of settings relevant to asthma-related immunophenotypes[24,25], with the perceived role of IFNs generally interpreted in the context of host responses to microbial triggers of acute exacerbations. However, we[25] and others have also shown[26,27] that Type1-IFNs negatively control many of the downstream pro-inflammatory effects of Th2 cytokines, including the IL4/IL13-induced stimulation of expression of receptors governing the endocytic, trafficking, and IgE-binding properties of myeloid cells[25]. It is thus conceivable that this late-stage rewiring of the network during prolonged maintenance SCIT, resulting in the introduction of coordinated Type1-IFN signalling into the aeroallergen-specific Th-memory-associated response profile, may provide a last-line-of-defence to stabilise immunotherapy via targeting key functions of activated Th2-memory cells that evade control via T-regulatory cells and related mechanisms. Given that the primary source of Type1-IFNs are myeloid cells (particularly DC), the findings above suggest that some of the long-term effects of SCIT may include modulation of the capacity of allergen-specific-Th-memory-cells to chemoattract/cluster-with/stimulate myeloid cells that are present within the microenvironment of the Th-memory cells during their interaction with aeroallergen. There are several earlier studies reporting SIT-associated effects on myeloid functions, including Type1-IFN response capacity of DC[28-30]. It is also relevant to note parallel findings from our earlier studies[31] contrasting the allergen-specific Th2-memory-associated co-expression network in HDM-sensitised atopic children with its counterpart underlying childhood responses to the highly Th2-polarising Diphtheria-tetanus-acellular-pertussis(DTaP) vaccine, the administration of which does not provoke Th2-associated allergic inflammation despite frequent stimulation of high levels of vaccine-antigen-specific IgE[32]. Mirroring the post SCIT-findings above, the clinically benign Th2-polarised DTaP-specific Th-memory-associated response also included upregulation of a prominent Type1-IFN-associated gene subnetwork, which was not observed in the corresponding allergen-specific network response[31].

This exploratory study has limitations including sample size, lack of a placebo control group, and non-availability of data on Th-memory-associated profiles in Yr3 during SCIT, which require

addressing in follow-ups. Importantly, the same network analytic approach needs to be applied to other immunotherapeutic treatments as SCIT may not be representative of all forms of desensitisation. Notwithstanding these limitations, the study for the first time introduces the concept that remodelling of overall allergen-specific Th-memory-associated response network topology, as opposed to solely quantitative effects on expression of regulatory/effector genes within the response network, may be central to the efficacy of allergen-specific immunotherapeutic treatment modalities. Rapidly emerging single-cell RNA-Seq technology provides an avenue for elucidation of these network interactions with higher precision than was possible in this study, and their application may open up new possibilities for therapeutic design relevant to allergy control.

REFERENCES

1. Akdis CA, Akdis M. Advances in allergen immunotherapy: aiming for complete tolerance to allergens. Sci Transl Med. 2015;7(280):280ps6.
2. Akdis M, Akdis CA. Mechanisms of allergen-specific immunotherapy: multiple suppressor factors at work in immune tolerance to allergens. J Allergy Clin Immunol. 2014;133(3):621-31.
3. Globinska A, Boonpiyathad T, Satitsuksanoa P, Kleuskens M, van de Veen W, Sokolowska M, Akdis M. Mechanisms of allergen-specific immunotherapy: Diverse mechanisms of immune tolerance to allergens. Ann Allergy Asthma Immunol. 2018;121(3):306-12.
4. Shamji MH, Durham SR. Mechanisms of allergen immunotherapy for inhaled allergens and predictive biomarkers. J Allergy Clin Immunol. 2017;140(6):1485-98.
5. Bosco A, McKenna KL, Devitt CJ, Firth MJ, Sly PD, Holt PG. Identification of novel Th2-associated genes in T memory responses to allergens. Journal of immunology (Baltimore, Md : 1950). 2006;176(8):4766-77.
6. Troy NM, Hollams EM, Holt PG, Bosco A. Differential gene network analysis for the identification of asthma-associated therapeutic targets in allergen-specific T-helper memory responses. BMC Med Genomics. 2016;9:9.
7. Bosco A, McKenna KL, Firth MJ, Sly PD, Holt PG. A network modeling approach to analysis of the Th2 memory responses underlying human atopic disease. Journal of immunology. 2009;182(10):6011-21.
8. Blumberga G, Groes L, Dahl R. SQ-standardized house dust mite immunotherapy as an immunomodulatory treatment in patients with asthma. Allergy. 2011;66(2):178-85.
9. Bufe A, Eberle P, Franke-Beckmann E, Funck J, Kimmig M, Klimek L, Knecht R, Stephan V, Tholstrup B, Weisshaar C, Kaiser F. Safety and efficacy in children of an SQ-standardized grass allergen tablet for sublingual immunotherapy. J Allergy Clin Immunol. 2009;123(1):167-73 e7.
10. Heaton T, Rowe J, Turner S, Aalberse RC, de Klerk N, Suriyaarachchi D, Serralha M, Holt BJ, Hollams E, Yerkovich S, Holt K, Sly PD, Goldblatt J, Le Souef P, Holt PG. An immunoepidemiological approach to asthma: identification of in-vitro T-cell response patterns associated with different wheezing phenotypes in children. Lancet. 2005;365(9454):142-9.
11. Dai M, Wang P, Boyd AD, Kostov G, Athey B, Jones EG, Bunney WE, Myers RM, Speed TP, Akil H, Watson SJ, Meng F. Evolving gene/transcript definitions significantly alter the interpretation of GeneChip data. Nucleic Acids Res. 2005;33(20):e175.
12. Kauffmann A, Gentleman R, Huber W. arrayQualityMetrics--a bioconductor package for quality assessment of microarray data. Bioinformatics (Oxford, England). 2009;25(3):415-6.

13. Irizarry RA, Hobbs B, Collin F, Beazer-Barclay YD, Antonellis KJ, Scherf U, Speed TP. Exploration, normalization, and summaries of high density oligonucleotide array probe level data. Biostatistics. 2003;4(2):249-64.

14. Lu J, Kerns RT, Peddada SD, Bushel PR. Principal component analysis-based filtering improves detection for Affymetrix gene expression arrays. Nucleic Acids Res. 2011;39(13):e86.

15. Ritchie ME, Phipson B, Wu D, Hu Y, Law CW, Shi W, Smyth GK. limma powers differential expression analyses for RNA-sequencing and microarray studies. Nucleic Acids Res. 2015;43(7):e47.

16. Leek JT, Johnson WE, Parker HS, Jaffe AE, Storey JD. The sva package for removing batch effects and other unwanted variation in high-throughput experiments. Bioinformatics (Oxford, England). 2012;28(6):882-3.

17. Miller JA, Horvath S, Geschwind DH. Divergence of human and mouse brain transcriptome highlights Alzheimer disease pathways. Proc Natl Acad Sci U S A. 2010;107(28):12698-703.

18. Shannon P, Markiel A, Ozier O, Baliga NS, Wang JT, Ramage D, Amin N, Schwikowski B, Ideker T. Cytoscape: a software environment for integrated models of biomolecular interaction networks. Genome Res. 2003;13(11):2498-504.

19. Breuer K, Foroushani AK, Laird MR, Chen C, Sribnaia A, Lo R, Winsor GL, Hancock RE, Brinkman FS, Lynn DJ. InnateDB: systems biology of innate immunity and beyond--recent updates and continuing curation. Nucleic Acids Res. 2013;41(Database issue):D1228-33.

20. Krämer A, Green J, Pollard J, Jr., Tugendreich S. Causal analysis approaches in Ingenuity Pathway Analysis. Bioinformatics (Oxford, England). 2014;30(4):523-30.

21. Yu H, Kim PM, Sprecher E, Trifonov V, Gerstein M. The importance of bottlenecks in protein networks: correlation with gene essentiality and expression dynamics. PLoS Comput Biol. 2007;3(4):e59.

22. Jutel M, Agache I, Bonini S, Burks AW, Calderon M, Canonica W, Cox L, Demoly P, Frew AJ, O'Hehir R, Kleine-Tebbe J, Muraro A, Lack G, Larenas D, Levin M, Nelson H, Pawankar R, Pfaar O, van Ree R, Sampson H, Santos AF, Du Toit G, Werfel T, Gerth van Wijk R, Zhang L, Akdis CA. International consensus on allergy immunotherapy. J Allergy Clin Immunol. 2015;136(3):556-68.

23. Penagos M, Eifan AO, Durham SR, Scadding GW. Duration of Allergen Immunotherapy for Long-Term Efficacy in Allergic Rhinoconjunctivitis. Curr Treat Options Allergy. 2018;5(3):275-90.

24. Bosco A, Ehteshami S, Panyala S, Martinez FD. Interferon regulatory factor 7 is a major hub connecting interferon-mediated responses in virus-induced asthma exacerbations in vivo. J Allergy Clin Immunol. 2012;129(1):88-94.

25. Subrata LS, Bizzintino J, Mamessier E, Bosco A, McKenna KL, Wikstrom ME, Goldblatt J, Sly PD, Hales BJ, Thomas WR, Laing IA, LeSouef PN, Holt PG. Interactions between innate antiviral

and atopic immunoinflammatory pathways precipitate and sustain asthma exacerbations in children. Journal of immunology (Baltimore, Md : 1950). 2009;183(4):2793-800.

26. Huber JP, Gonzales-van Horn SR, Roybal KT, Gill MA, Farrar JD. IFN-alpha suppresses GATA3 transcription from a distal exon and promotes H3K27 trimethylation of the CNS-1 enhancer in human Th2 cells. Journal of immunology (Baltimore, Md : 1950). 2014;192(12):5687-94.

27. Huber JP, Ramos HJ, Gill MA, Farrar JD. Cutting edge: Type I IFN reverses human Th2 commitment and stability by suppressing GATA3. Journal of immunology (Baltimore, Md : 1950). 2010;185(2):813-7.

28. Gueguen C, Bouley J, Moussu H, Luce S, Duchateau M, Chamot-Rooke J, Pallardy M, Lombardi V, Nony E, Baron-Bodo V, Mascarell L, Moingeon P. Changes in markers associated with dendritic cells driving the differentiation of either TH2 cells or regulatory T cells correlate with clinical benefit during allergen immunotherapy. J Allergy Clin Immunol. 2016;137(2):545-58.

29. O'Mahony L, Akdis CA, Eiwegger T. Innate mechanisms can predict successful allergy immunotherapy. J Allergy Clin Immunol. 2016;137(2):559-61.

30. Tversky JR, Bieneman AP, Chichester KL, Hamilton RG, Schroeder JT. Subcutaneous allergen immunotherapy restores human dendritic cell innate immune function. Clin Exp Allergy. 2010;40(1):94-102.

31. White OJ, McKenna KL, Bosco A, van den Biggelaar AHJ, Richmond P, Holt PG. A genomics-based approach to assessment of vaccine safety and immunogenicity in children. Vaccine. 2012;30:1865-74.

32. Ryan EJ, Nilsson L, Kjellman N, Gothefors L, Mills KH. Booster immunization of children with an acellular pertussis vaccine enhances Th2 cytokine production and serum IgE responses against pertussis toxin but not against common allergens. Clin Exp Immunol. 2000;121(2):193-200.

Table I. Activation Z-scores at each visit for the V5 upstream drivers.

Upstream regulators	V1	V2	V4	V5
NFkB (complex)	5.80	5.85	5.84	7.05
IL1B	6.08	5.80	5.87	6.87
CD40LG	5.74	5.94	6.04	6.50
TCR (complex)	6.66	5.85	6.61	6.28
IL2	6.79	6.66	6.69	6.20
IL7	5.32	5.78	5.27	6.14
TNF	5.58	5.12	5.32	6.10
MYC	5.97	5.75	6.36	6.07
IFNA2	1.65	1.79	0.55	**5.99**
IRF7	0.60	1.95	-0.16	**5.85**
IFNG	3.48	3.93	2.60	**5.78**
TLR4	4.71	4.80	4.11	5.62
IL15	5.24	5.29	5.62	5.54
MYCN	4.02	4.41	4.65	5.35
TLR9	4.76	4.69	3.81	5.00
STAT1	2.27	3.04	1.86	**4.87**
IL18	4.53	4.56	4.46	4.78
CSF2	4.71	4.12	4.32	4.25
IL5	4.22	4.15	4.17	4.02
Immunoglobulin (complex)	2.85	3.37	3.71	3.96
CD3 (complex)	3.52	3.62	3.68	3.96
IL3	3.67	3.63	3.39	3.86
STAT3	3.32	3.37	3.04	2.65
IL27	1.96	1.79	1.00	2.28
IL4	2.49	2.44	2.53	2.19
IL10	-2.23	-2.48	-2.81	-2.85
CD28	-5.38	-4.97	-5.14	-4.49
BCL6	-4.91	-4.93	-4.82	-4.94
RICTOR	-3.64	-4.95	-4.35	-5.14
OSM	3.14	2.85	3.04	4.63

Putative regulators of the DEG were identified at each visit employing Ingenuity Systems Upstream Regulator Analysis. Molecular drivers with Benjamini & Hochberg adjusted *P-values*≤0.05 and absolute *Z-scores*≥2.0 were deemed significant (positive *Z-scores*=activation, negative *Z-scores*=inhibition).

FIGURE LEGENDS

Figure 1. Evolution of symptoms over time during SCIT.

Normalised respiratory symptom scores based on symptoms recorded for one week prior to visit dates were plotted (as mean ± 95%CI) for pre-(V1) and post-SCIT treatment (V2/3.5mths, V4/12mths, V5/24mths and V6/36mths sampling points.

Figure 2. CD4+ T-cell immune responses pre-treatment (V1) were correlated with respiratory symptoms.

A) Volcano plot showing HDM-specific DEG at V1 (dashed horizontal line=adjusted *p-value*<0.05; n=25). B) Pathways analysis of DEG was carried out with InnateDB (black=upregulated pathways, open=downregulated pathways). C) Predicted upstream regulators of the DEG (black=activated drivers, open=inhibited drivers). LPS=lipopolysaccharide. D) It was tested if response to stimulation is associated with respiratory symptoms at V1 employing *limma* and volcano plot shows the correlation of respiratory symptoms with CD4+T cell responses at V1 (n=25); E) corresponding up-and-downregulated pathways and F) upstream regulators.

Figure 3. CD4+ T-cell responses over the course of SCIT treatment (V2, V4 and V5).

A) Volcano plots showing HDM-specific CD4+ T-cell responses at V2, V4 and V5 respectively (n=25). The dashed horizontal line indicates an adjusted *p-value*<0.05. B) Pathways analysis of DEG was carried out with InnateDB (black=upregulated pathways[includes IFN signaling/striped at V5], open=downregulated pathways). C) Predicted upstream regulators of the DEG (black=activated drivers, open= inhibited drivers).

Figure 4. Network analysis of the HDM-induced T cell responses.

Co-expression networks were constructed employing *WGCNA* (n=25, V1/V2/V4; n=24, V5). A) Network connectivity patterns(V2/V4/V5) were superimposed over V1 modular architecture. B) Comparison of V1 modular architecture with the module assignments V2/V4/V5 (left panel). Roadmap showing progressive re-wiring of the modules (A-N) over the course of SCIT(right panel; black circles/lines=differentially expressed, grey=not differentially expressed. C) Box-and-whisker plots showing modules with DEG. Median adjusted *p-values:* * <0.05,** <0.01,*** <0.001,**** <0.0001.

Figure 5. Reconstruction of the network wiring diagram at V1/V5 reveals changes in network connectivity.

Co-expression networks were constructed employing *WGCNA* and visualised in Cytosape (n=25, V1; n=24, V5). The top-800 network edges/pairwise connections were utilised for network reconstruction. We repeated this analysis with a different number of edges (e.g. 300, 500, 800, 1000, 1500) and the data were unchanged. The node size reflects the number of connections per gene. Node colour spectrum in key (red-blue) designates positive-to-negative log2FC; note module A is not upregulated until V5.

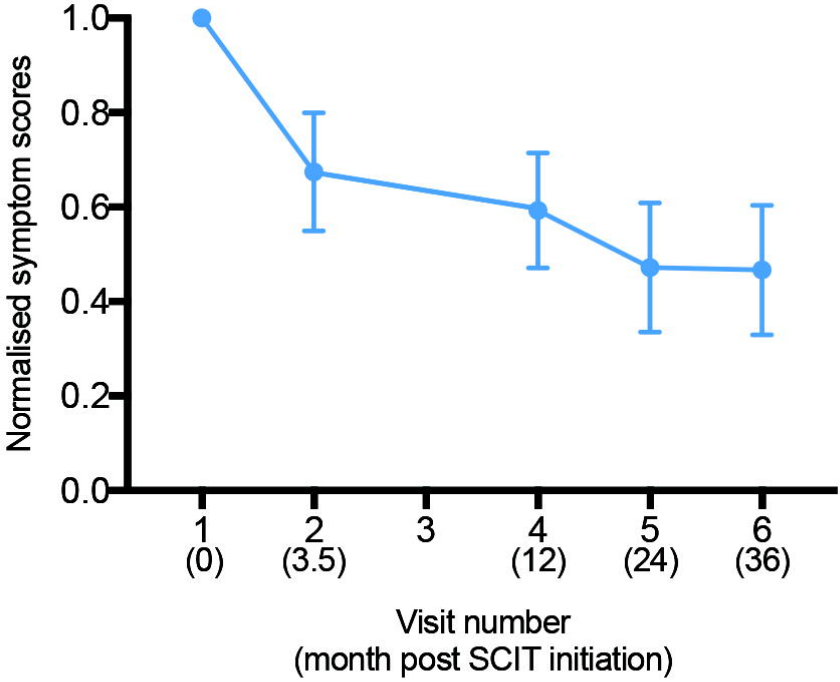
1.0
0.8
0.6
0.4
0.2
0.0
Normalised symptom scores
1
(0)
2
(3.5)
3
4
(12)
5
(24)
6
(36)
Visit number
(month post SCIT initiation)

Figure 1

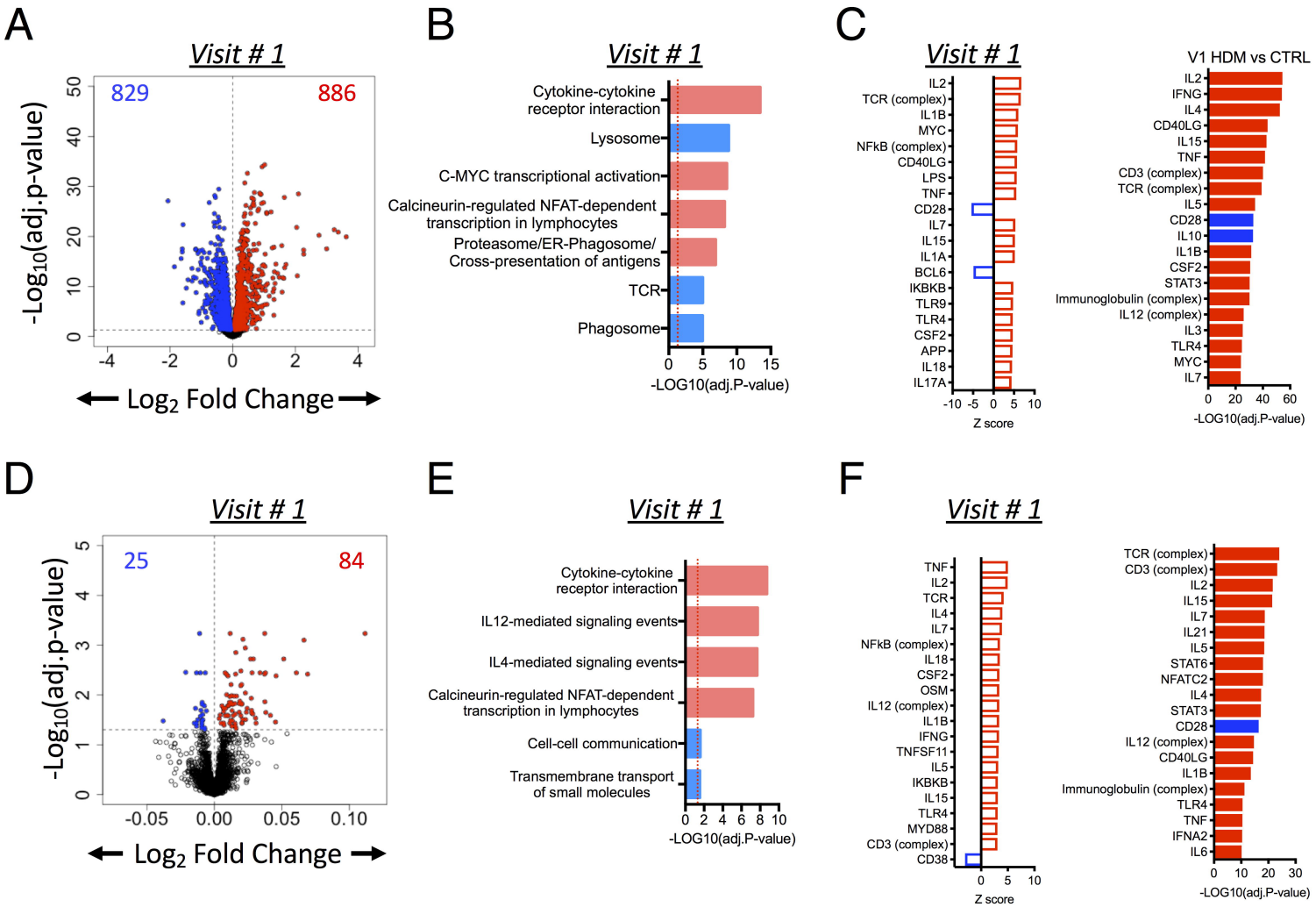
A
Visit # 1
829
886
-Log10(adj.p-value)
Log2 Fold Change
B
Visit # 1
Cytokine-cytokine receptor interaction
Lysosome
C-MYC transcriptional activation
Calcineurin-regulated NFAT-dependent transcription in lymphocytes
Proteasome/ER-Phagosome/ Cross-presentation of antigens
TCR
Phagosome
-LOG10(adj.P-value)
C
Visit # 1
IL2
TCR (complex)
IL1B
MYC
NFkB (complex)
CD40LG
LPS
TNF
CD28
IL7
IL15
IL1A
BCL6
IKBKB
TLR9
TLR4
CSF2
APP
IL18
IL17A
Z score
V1 HDM vs CTRL
IL2
IFNG
IL4
CD40LG
IL15
TNF
CD3 (complex)
TCR (complex)
IL5
CD28
IL10
IL1B
CSF2
STAT3
Immunoglobulin (complex)
IL12 (complex)
IL3
TLR4
MYC
IL7
-LOG10(adj.P-value)
D
Visit # 1
25
84
-Log10(adj.p-value)
Log2 Fold Change
E
Visit # 1
Cytokine-cytokine receptor interaction
IL12-mediated signaling events
IL4-mediated signaling events
Calcineurin-regulated NFAT-dependent transcription in lymphocytes
Cell-cell communication
Transmembrane transport of small molecules
-LOG10(adj.P-value)
F
Visit # 1
TNF
IL2
TCR
IL4
IL7
NFkB (complex)
IL18
CSF2
OSM
IL12 (complex)
IL1B
IFNG
TNFSF11
IL5
IKBKB
IL15
TLR4
MYD88
CD3 (complex)
CD38
Z score
TCR (complex)
CD3 (complex)
IL2
IL15
IL7
IL21
IL5
STAT6
NFATC2
IL4
STAT3
CD28
IL12 (complex)
CD40LG
IL1B
Immunoglobulin (complex)
TLR4
TNF
IFNA2
IL6
-LOG10(adj.P-value)

Figure 2

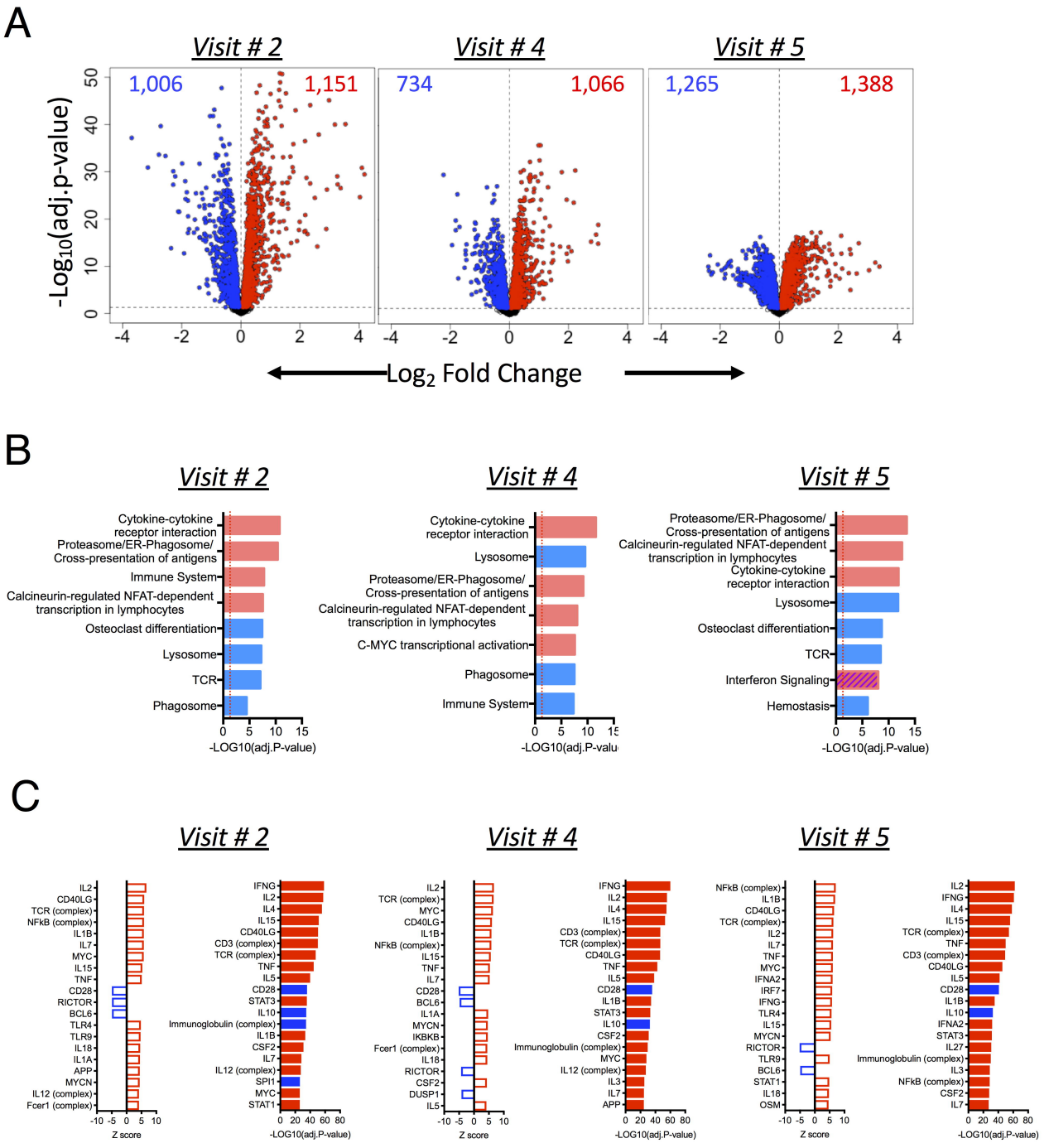
A
Visit # 2
Visit # 4
Visit # 5
1,006
1,151
734
1,066
1,265
1,388
-Log10(adj.p-value)
Log2 Fold Change
B
Visit # 2
Cytokine-cytokine receptor interaction
Proteasome/ER-Phagosome/ Cross-presentation of antigens
Immune System
Calcineurin-regulated NFAT-dependent transcription in lymphocytes
Osteoclast differentiation
Lysosome
TCR
Phagosome
-LOG10(adj.P-value)
Visit # 4
Cytokine-cytokine receptor interaction
Lysosome
Proteasome/ER-Phagosome/ Cross-presentation of antigens
Calcineurin-regulated NFAT-dependent transcription in lymphocytes
C-MYC transcriptional activation
Phagosome
Immune System
Visit # 5
Proteasome/ER-Phagosome/ Cross-presentation of antigens
Calcineurin-regulated NFAT-dependent transcription in lymphocytes
Cytokine-cytokine receptor interaction
Lysosome
Osteoclast differentiation
TCR
Interferon Signaling
Hemostasis
C
Visit # 2
Visit # 4
Visit # 5
Z score
-LOG10(adj.P-value)

Figure 3

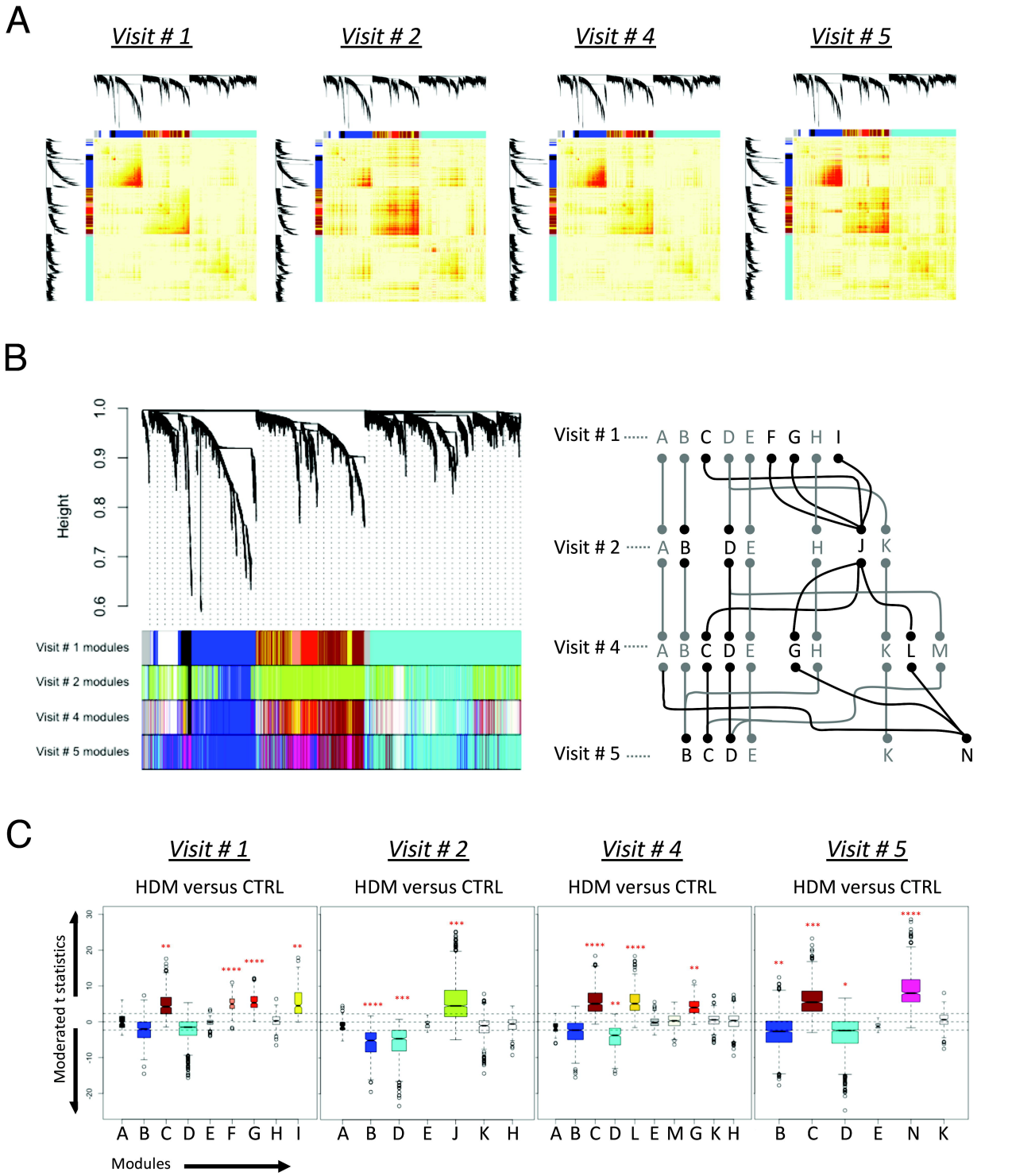

Module Legend			
A	Type 1 interferon – not differentially expressed	**H**	FAS signaling – not differentially expressed
B	Lysosome/phagosome/antigen processing & presentation	**I**	IL2 signaling / Foxp3
C	Ribosome/Translation/Metabolism of proteins	**J**	Th2, inflammation/proteasome/phagosome & cytokine receptor interaction, metabolism of proteins, IL2 signalling/Foxp3,
D	TCR signaling	**K**	Transcription & IL6 signalling – not differentially expressed
E	Unassigned/unclustered genes – not differentially expressed	**L**	Th2, proteasome/phagosome & cytokine receptor interaction, metabolism of proteins, IL2 signalling/Foxp3
F	Th2	**M**	Ribosomal translation – not differentially expressed
G	Inflammation/chemokine & cytokine receptor interactions/phagosome/proteasome	**N**	Th2, inflammation/proteasome/phagosome & cytokine receptor interaction, metabolism of proteins, IL2 signaling/Foxp3, **type 1 interferon**

Median adj. p-value: * = 0.05, ** = 0.01, *** = 0.001, **** = 0.0001

Figure 4

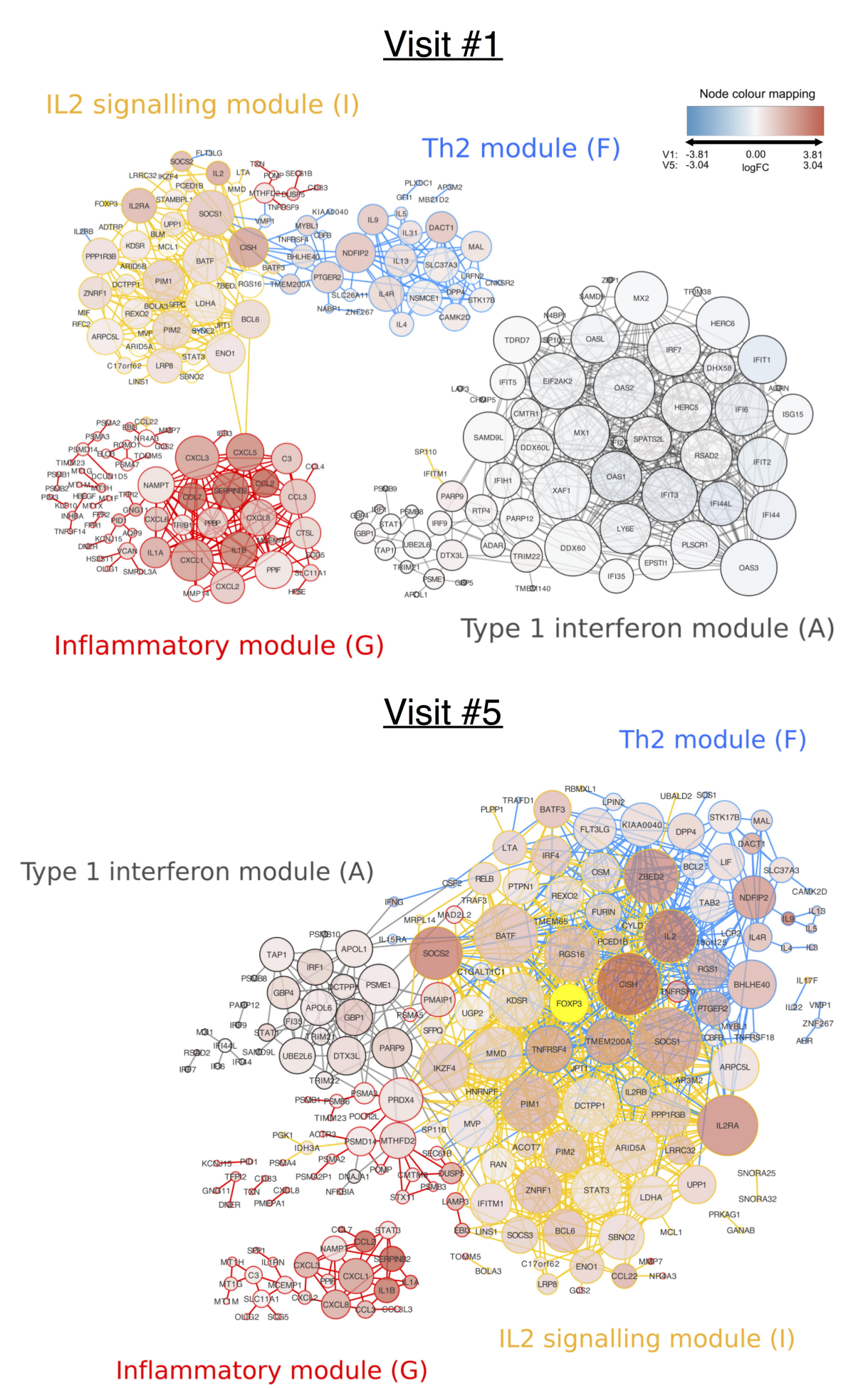
Visit #1
IL2 signalling module (I)
Th2 module (F)
Node colour mapping
V1: -3.81 0.00 3.81
V5: -3.04 logFC 3.04
Inflammatory module (G)
Type 1 interferon module (A)
Visit #5
Th2 module (F)
Type 1 interferon module (A)
IL2 signalling module (I)
Inflammatory module (G)

Figure 5